HHS Public Access

Author manuscript

Ann Biomed Eng. Author manuscript; available in PMC 2017 August 11.

Published in final edited form as:

Ann Biomed Eng. 2012 January ; 40(1): 23–36. doi:10.1007/s10439-011-0390-6.

Dynamic Changes in Neural Circuit Topology Following Mild Mechanical Injury *In Vitro*

Tapan P. Patel[1], **Scott C. Ventre**[1], and **David F. Meaney**[1,2]

[1]Department of Bioengineering, University of Pennsylvania, 220 S 33rd St, Philadelphia, PA 19104, USA

[2]Department of Neurosurgery, University of Pennsylvania, Philadelphia, PA 19104, USA

Abstract

Despite its enormous incidence, mild traumatic brain injury is not well understood. One aspect that needs more definition is how the mechanical energy during injury affects neural circuit function. Recent developments in cellular imaging probes provide an opportunity to assess the dynamic state of neural networks with single-cell resolution. In this article, we developed imaging methods to assess the state of dissociated cortical networks exposed to mild injury. We estimated the imaging conditions needed to achieve accurate measures of network properties, and applied these methodologies to evaluate if mild mechanical injury to cortical neurons produces graded changes to either spontaneous network activity or altered network topology. We found that modest injury produced a transient increase in calcium activity that dissipated within 1 h after injury. Alternatively, moderate mechanical injury produced immediate disruption in network synchrony, loss in excitatory tone, and increased modular topology. A calcium-activated neutral protease (calpain) was a key intermediary in these changes; blocking calpain activation restored the network nearly completely to its pre-injury state. Together, these findings show a more complex change in neural circuit behavior than previously reported for mild mechanical injury, and highlight at least one important early mechanism responsible for these changes.

Keywords

Traumatic brain injury; Concussions; Calcium indicator dyes; Stochastic integrate-and-fire model; Neural network; Synchrony; Cluster; Excitatory tone; Calpain

INTRODUCTION

Concussions are a form of mild traumatic brain injury that represents at least 80% of the traumatic brain injuries occurring each year in the United States.[24] Although often associated with sports, the majorities of concussions occur outside of sporting activities and include motor vehicle accidents, falls, and any situation involving sudden acceleration or

Address correspondence to David F. Meaney, Department of Bioengineering, University of Pennsylvania, 220 S 33rd St, Philadelphia, PA 19104, USA. dmeaney@seas.upenn.edu.

CONFLICT OF INTEREST

The authors do not have any conflict of interest.

deceleration of the head. Long considered an injury that was ‘inevitable’ with little recourse, the growing awareness of the long-term effects of concussion led to a renewed focus on understanding, preventing, and treating concussions. New technology to assess the mechanical circumstances of concussions is leading to a new perspective on effective protective equipment. Alongside the advances in basic science understanding of concussions, new diagnostic imaging methods are also becoming available to better evaluate and assist clinicians in the care of patients with a concussion.[14]

The cellular substrate of concussion is largely unknown.[36] One theory on the mechanical origin of concussions proposes that the cortical strains appearing in the gray matter at the moment of injury are the most likely reason for the impairments that occur in a concussion.[46] Alternatively, others pose that deformation of the brainstem structures are key in producing the brief periods of unconsciousness associated with severe concussion.[6,55] A common theme among these concussion theories is that the mechanical energy during rapid head motions will deform brain tissue and, ultimately, the cellular ensembles that form these tissues. However, at the multicellular scale, it is not clear if these transient mechanical events will cause permanent changes in the neuronal morphology or, alternatively, the wiring of neural circuits within brain regions associated with concussion. These changes in both the neuronal connections and, alternatively, the wiring of neural networks can play a key role in the recovery of the brain following a concussion.

Several *in vitro* models of injury have been designed to investigate the response of the brain parenchyma to mechanical stimulus in isolation, without confounders such as vascular damage, systemic inflammation, fluctuations in pH, temperature, oxygenation level or intracranial pressure.[38,40] Examples of such models include the transection model,[41,42] the compression or weight-drop model,[10,53] the hydrostatic pressure[43] or hydrodynamic model,[28] shear strain models,[4,25] and several stretch injury models.[34,39,49] Of these, the stretch injury or substrate deformation model captures essential features of the biomechanics of an *in vivo* brain deformation in concussions.

Along with advances in animal and *in vitro* models of injury, there has been a concerted effort to start mapping the connections among neurons within the brain for both small and large organisms. In parallel, a substantial new set of tools appeared for formulating principles of information flow among neural networks, measuring their relative connectivity map, and understanding key points of control for complex net-works.[7,9,18,33,50,57] Key in this progress is a new emerging set of fluorescent reagents that provide stable, long-term optically based recording of dissociated neurons, ensembles of neurons within acute brain slices, and the living cortex.[15,37,60] Collectively, these new tools allow for the direct visualization of the nervous system at an unprecedented scale—it allows one to estimate the input/output connectivity maps among neurons, assess the relative strength of connections among neurons in a network, and to define the network scaling principles used in the design of the network.

In this study, we critically analyze fluorescence based imaging methods for mapping neural network properties, and use this analysis to design experiments for measuring changes in network behavior following mild and moderate stretch injury to cortical neuronal networks

in vitro. Unlike higher injury levels (>80% stretch) that will cause neuronal death within 24 h post-injury, we find that mild levels of mechanical injury (35% stretch) causes widespread changes in network topology, synchrony, and excitatory transmission. The network that was once highly interconnected prior to injury breaks off into multiple, smaller clusters of locally connected modules. Long-range synaptic transmission is impaired. Functionally, there is a significant drop in network synchrony. At these stretch levels, there is delayed proteolysis of voltage gated sodium channels, mediated by the calcium sensitive protease, calpain.[62] We show that pharmacological blockade of calpain improves network synchrony. Interestingly, calcium influx through the NMDA receptor is critical in mediating some, but not all, of these changes. Alternatively, even milder mechanical injury (10% stretch) produced very little changes in network topology or synchrony, however, there was a brief period of heightened spontaneous activity following injury.

MATERIALS AND METHODS

In Silico Simulation of Network Behavior

We used a stochastic integrate-and-fire model to evaluate network dynamics, predict alterations in cytosolic calcium, and use these estimates of cytosolic calcium to predict measurements derived from fluorescent indicator dyes and genetically encoded calcium indicators (see Simulating Calcium Dynamics). Each neuron within the model is designated as either an inhibitory (*I*) or excitatory (*E*) neuron. We base this model on previous models for network behavior, which contain neurons that show either a regular spiking (RS) or intrinsic bursting (IB) behavior.[17] When modeled as a regular spiking neuron, the membrane potential of a single neuron will receive a spiking input, followed by a refractory period defined by a monoexponential decay. To monitor changes in membrane potential *v(t)*, we also include a leak current, a calcium sensitive hyperpolarizing current for potassium channels ($I_{K(Ca)}$), a noise component, and a generalized formulation of the synaptic current:

$$C\frac{\mathrm{dv}}{\mathrm{dt}}=I_{\mathrm{leak}}+I_{\mathrm{spike}}+I_{\mathrm{K(Ca)}}+I_{\mathrm{noise}}+I_{\mathrm{syn}},$$

where C is the overall capacitance of neuronal membrane. The synaptic current has contributions from both the AMPA and NMDA receptors,

$$I_{\mathrm{syn}}=d_j(I_{\mathrm{AMPA}}+I_{\mathrm{NMDA}}),$$

where d_j is a synaptic depression factor that accounts for the loss of vesicles from the j pre-synaptic terminals. AMPA and NMDA currents are computed from previous *Smoldyn* simulations that give a temporal profile of the number of open receptors (N_{AMPA} and N_{NMDA}), following synaptic vesicular release[54]:

$$I_{\mathrm{AMPA}}=g_{\mathrm{AMPA}}\times(V_{\mathrm{m}}-E)\times N_{\mathrm{AMPA}},$$

$$I_{\mathrm{NMDA}} = g_{\mathrm{NMDA}} \times (V_{\mathrm{m}} - E) \times N_{\mathrm{NMDA}},$$

where g_{AMPA} = 12 pS, g_{NMDA} = 45 pS, and the reversal potential E = 0. The remainder of model parameters are consistent with.[17]

For an intrinsic bursting neuron, we follow French *et al.* and add a low threshold calcium channel to augment the existing components incorporated for a bursting neuron. By incorporating the stochastic nature of **AMPA** and **NMDA** receptor opening, we enhance the previous model and account for the observed variability in activity patterns.

Defining the Connectivity of the In Silico Network

The connectivity of our *in silico* model was prescribed to match *in vitro* neural network development. Past work using dissociated cortical neurons indicate that the input and output degree distribution is Poisson.[1,61] In selecting targets for neuron *i*'s outputs, we utilized a weighted random sampling function, where neurons closest to, and in the direction of *i*'s axonal growth cone are preferentially connected. The number, or degree, of inputs (Ki) and outputs (Ko), and the relative distribution of the degree among an ensemble of neurons, defines the overall connectivity in the neural circuit. Models of cortical neural networks were developed and executed using a custom MATLAB script (Mathworks, Inc.). We simulated the activity of 100 neurons for 10 s, with 2-ms timesteps, and average Ki = Ko = 20, where each connection was further divided into 20–50 synapses for a total of ~10,000 synapses. Synapses were populated with 80 AMPARs and 20 NMDARs. Simulations ran for 3 h in simulation time to correspond with 10 s of imaging data.

Simulating Calcium Dynamics

Calcium influx is simulated by incorporating a step in free cytosolic calcium with each action potential, followed by an exponential decay. Calcium traces were used to predict changes in the fluorescence of two commonly used calcium indicator dyes, fura-2 and fluo-4. Predicted fluorescence is dependent on a combination of the buffering property of the indicator (see Table 1), the acquisition rate of the imaging camera (0.4–20 frames per second; see methods below), and the sensitivity of the detector. The fluorescence, R, was determined from:

$$[\mathrm{Ca}^{2+}] = \frac{R - R_{\mathrm{min}}}{R_{\mathrm{max}} - R} \times K_{\mathrm{d}}$$

and then downsampled to match experimental imaging speeds. R_{min} was determined by imaging neurons in a calcium free saline solution and R_{max} was determined by imaging neurons in normal saline solution, exposed to 5 μM ionomycin (Sigma-Aldrich). The fraction of action potentials that was resolved by the calcium indicator dye was used to compare different imaging conditions.

Cell Culture

Animal procedures were performed in accordance with the Institutional Animal Care and Use Committee at the University of Pennsylvania. We used previous methods developed in our group to generate mixed cultures of neurons/glia from embryonic day 18 rats (E18; Charles River, Wilmington, MA).[56] Cell suspensions isolated from embryonic rats were plated directly onto treated silicone substrates (Sylgard 184 + 186 mix, Dow Corning, Midland, MI). Neurons were cultured for 18–21 days in Neurobasal media (Invitrogen) with B27 and Glutamax (Gibco) in a humidified incubator at 37 °C, 5% CO_2. The length of time for culturing was used to allow for the full expression of glutamate receptors.[20]

Drug Treatments

All compounds were solubilized in controlled saline solution (CSS; in mM: 120 NaCl, 5.4 KCl, 1 $MgCl_2$, 1.8 $CaCl_2$, 25 HEPES, 15 glucose, pH 7.3), added to the cells 5 min prior to injury, and remained on the cultures for the duration of the experiment unless otherwise noted. Cortical neurons were incubated in bicuculline methobromide 50 μM (Tocris), APV 25 μM (Tocris), or MDL28170 50 μM (Calbiochem) as needed.

Mechanical Injury of Cortical Neurons

Cortical neurons at 18–21 days *in vitro* (DIV) on flexible membranes were placed on a stainless steel plate and covered with a top plate to form a sealed chamber. Increasing the chamber pressure to its peak level in 15 ms caused the compliant silicone membrane to stretch, in turn applying a stretch to the cultured neurons. This pressurization phase was immediately followed by a release of the pressure, typically within 25 ms of achieving the peak pressure. Although cells were cultured over a circular area (23 mm diameter), we designed the supporting stainless steel plate to expose only cells in a defined region (a 3 mm × 18 mm rectangular region; approximately 1/3 of the culture surface area) to a stretch, designing the system to provide a uniform membrane stretch over 95% of the surface within that region.[34] The membrane in the injured region was stretched uniaxially, where the width was extended 10% (mild) or 35% (moderate) beyond its initial width before returning to its original dimension. We did not observe any obvious detachment of the cells from the membrane following stretch injury, nor did we observe any gross morphological changes in the cultures. This stretch level does not cause a significant increase in cell death compared to unstretched controls.[35] Naïve unstretched neurons served as reference conditions for statistical comparison.

Calcium Imaging

Three distinct calcium indicators were used in our experiments. The ratiometric dye Fura-2AM (Molecular Probes, Eugene, OR; 5 μM) was incubated with each culture for 45 min at 37 °C in CSS, supplemented with $NaHCO_3$ 26 mM. In separate experiments, the single emission indicator Fluo-4 (2 μM) was loaded into cells at 37 °C for 30 min. For imaging the long-term changes in network activity following mechanical injury, cells were transduced with a virus expressing the genetically encoded calcium indicator GCaMP3 (AAV2/1-hSynapsin1-GCaMP3, UPenn vector core, Addgene #22692) at DIV 7, and the virus was allowed to express for 10 days before testing.[60]

Immediately prior to imaging, cultures were rinsed in buffered saline solution to remove any residual indicator dye and placed on a spinning disk microscope (CSU-10b, Solamere Technologies), configured on a Nikon TE2000 microscope (Optical Apparatus, Ardmore, PA). A CCD camera (Photometric Cool-Snap HQ2, BioVision, Exton PA) was used to capture images at a relatively high framing rate for both GCaMP3 and Fluo-4 labeled cells. Spontaneous calcium activity from −200 neurons in the field of view was recorded for 5 min, at 20 Hz acquisition speed using a 488-nm excitation laser and Nikon 10×/0.45 Plan Apo objective.

A subset of cultures comparing Fluo-4 and Fura-2 indicator dyes was tested on a TE300 microscope. For Fura-2 imaging, cells were alternately excited at 340 and 380 nm using an excitation shutter filter wheel (Sutter Instruments, Novato, CA) and the corresponding emission images (510 nm) were collected using a 14-bit Hamamatsu camera (model c4742-98; Optical Apparatus, Ardmore, PA) at a rate of one ratio image approximately every 2 s. Fluo-4 images were also collected at the same acquisition rate (0.4 Hz), and higher rates (1 and 10 Hz) for comparison purposes.

Imaging Analysis

Custom-coded MATLAB scripts were used to analyze the image stacks. Individual neurons in the field of view were identified and the mean fluorescence within each soma was computed across the image stack. High frequency noise was eliminated with a wavelet-based algorithm,[48] and peak detection algorithm identified the timestamps of calcium transient onset.[44] The timestamps were used to generate a raster plot, which provides a compact visual representation of the population activity over time.

Measurements of Synchrony and Network Topology

Synchronization of the network was evaluated using a previously published set of analysis methods, modified to include non-linear interactions.[30,51] Each neuron *j* has a discrete sequence of spike times, $t_j(n)$. We assigned a time-varying instantaneous phase to each neuron *j* within the nth inter-spike interval, given by:

$$\varphi_j(t,n)=2\pi n+2\pi\frac{t-t_j(n)}{t_j(n+1)-t_j(n)}.$$

The circular variance of the phase difference between pair-wise neurons *j* and *k*, given by:

$$S_{\mathrm{jk}}=\left|e^{i(\varphi_j(t)-\varphi_k(t)}\right|$$

was used to generate a phase synchronization matrix. An eigenvector based algorithm identified clusters of locally synchronized neurons and yielded a global synchronization index, which ranges from 0 (random, non-coordinated activity) to 1 (perfectly synchronous activity).[51] Functional connectivity was determined by using surrogate time-series to test for significant interactions between all pairs of neurons.[31] The modularity of the resulting

network, which ranges from 0 (no modules or community structure) to 1 (non-overlapping modules) was determined to describe changes in network topology.[45,50]

Excitatory tone in the network was determined using a modified approach of disintegrating the giant component.[5] Rather than using field stimulus and exposing neurons to large currents, we applied bicuculline and relied on the native excitatory circuitry to drive synchronous oscillations. By slowly adding increasing concentrations of AMPA receptor antagonist NBQX, we were able to stop synchronous oscillations and arrive at a critical value of [NBQX]/K_d that disintegrates the excitatory network[13] (K_d = 47 nm).

Statistics

Data were analyzed by ANOVA with Tukey's *post hoc* test. At least $n = 10$ cultures, from three different isolations were tested for each experimental condition.

RESULTS

In Silico Neural Network Yields Estimates of Optimal Imaging Parameters Necessary to Achieve Accurate Spike Detection

We first developed an *in silico* model of neural network activity, conducting a parametric analysis to understand advantages and drawbacks of choices that are commonly used in optical imaging of neural activity. Our network model used a weighted pseudo-randomized network connection topology, and individual synapses, populated with AMPA and NMDA receptors, were assumed to follow a stochastic activation pattern per a recent report[54] (Fig. 1a). Integration of current from individual synaptic release events, which could include a random vesicular release event (i.e., synaptic noise), showed development of spontaneous network activity that would vary temporally (Fig. 1b). Within individual neurons, these periodic bursts of activity would slightly precede or follow neighboring neurons, would show some modest diversity in the spontaneous timing of bursts. Repeat simulations of the same network topology yielded slightly different patterns of activity, owing to the stochastic synaptic activation scheme. Inhibitory neurons in the network provided modulation of the activity pattern, as reducing the relative strength of the inhibitory neuronal tone led to a progressive synchronization of network activity (Fig. 1c), resembling a common technique to synchronize the electrical activity of cortical neuron cultures *in vitro*.

Using estimates of calcium binding for different calcium indicator dyes, we investigated how well fura-2 and fluo-4 capture underlying electrical activity. Under the most ideal conditions, without hardware noise, we found neither Fura-2 nor Fluo-4 provided accurate estimates of precise timing of action potential firing when sampled at relatively low rates. Although Fura-2 offers approximately double the accuracy in detecting action potentials within networks under very low framing rate conditions (0.4 frames per second), the predicted accuracy was still less than 10% (Fig. 1d). Fluo-4 offers the ability, with its single emission wavelength, to capture fluorescence imaging data at a much faster rate limited only by the imaging hard-ware.[59] Across typical imaging rates available in commercial interline CCD and EMCCD camera, we find that image acquisition rate will substantially improve the fidelity between increases in calcium indicator fluorescence changes and action potential

activity (Fig. 1d). Optimal image acquisition rates with the Fluo-4 indicator exceed 80% accuracy in capturing action potentials (85 ± 7.8%) at reasonable framing rates, and approach 60% (58 ± 8.52) even at 10 frames per second.

Optical Imaging of Network Activity In Vitro Reveals Network Modules and Minimum Acquisition Requirements

We tested these *in silico* predictions directly on our imaging system, assessing both the relative performance of different indicator dyes at low framing rates and the performance of the Fluo-4 indicator at higher framing rates. Several algorithms are available to detect spike patterns from optical imaging data, and our wavelet-based algorithm yielded consistent, repeatable measures of activity on a single neuron basis that was not complicated by altering or changing threshold conditions and baseline shifts that are often challenging experimental factors (Figs. 2a, 2b). Applying this detection algorithm to neuronal network cultures (n = 10), we found no discernable difference between Fluo-4 and Fura-2 at framing rates typically used in time-lapse imaging applications (0.4 Hz) (Figs. 2c, 2d). In the same culture, we progressively increased framing acquisition rates using the Fluo-4 indicator dye. Acquiring images at 1 and 20 Hz, rather than 0.4 Hz, revealed a much more dynamic activity pattern, picking up many short lived calcium transients (Figs. 2d–2f). At higher imaging rates, we could no longer detect activity patterns clearly evident at lower framing rates, presumably due to the aggregate detection limits of the objective, filters, camera, and other optical elements in the light path. We observed no significant difference in the activity patterns measured with either Fluo-4 or GCaMP3, a recently introduced genetically engineered calcium sensor (data not shown).[60]

After establishing the necessary acquisition speeds to accurately detect activity, we next considered both the number of neurons and length of imaging time necessary to accurately estimate network synchronization, a key parameter often used to determine network modules.[3] Across multiple cultures (n = 8), we found that the phase difference in the calcium transients was not spatially sensitive, suggesting a randomized network topology often associated with dissociated cortical networks.[23] The periodic bursting behavior observed with neural networks, when acquired at high framing rates (20 Hz), yielded a synchronization index for the entire culture and also produced measures of smaller subclusters of neurons with highly coordinated firing activity (Figs. 3b, 3c). To obtain accurate measures of synchronization, we needed imaging data from at least 40 individual neurons to achieve less than 5% error (Fig. 3e). Similarly, we found that at least 2.5 min of imaging spontaneous calcium activity in the dissociated cultures was necessary to achieve reasonably stable estimates of the synchronization index (Fig. 3f).

A final parameter that we investigated experimentally is the excitatory tone of the network. Network disinhibition with bicuculline caused synchronized calcium oscillations (Fig. 4a) whose frequency was systematically reduced with increasing dose of AMPA receptor antagonist NBQX (Figs. 4b, 4c), until oscillations abruptly stopped at certain threshold [NBQX] (Fig. 4d). The $[\mathrm{NBQX}]_{\mathrm{threshold}}/K_{\mathrm{d}}$ was recorded as the excitatory tone. Similar to network synchronization, sampling from a large neuronal population may not be necessary to achieve accurate estimates of this parameter. Using a progressive inhibition of AMPA

receptors in dissociated culture, we found that the measured excitatory tone would require recording activity from at least 30 neurons to achieve a stable measure with less than 5% variation. Using this as a guide, we verified that excitatory tone was modulated across development time in the dissociated cultures. Several studies indicate a progressive increase in AMPA receptor number indicated with immunoblotting and immunocytochemistry,[32] and we found a similar increase in the excitatory tone that progressed and stabilized at later DIV (Fig. 4e).

Mechanical Injury to Cortical Neurons Changes Network Dynamics and Functional Connectivity

Upon establishing the necessary imaging conditions to capture accurate measures of network behavior, we next studied the response of cortical neurons to two distinct levels of mechanical injury. Neither level of mechanical injury causes neuronal death 24 h following injury.[35] One level of mechanical injury (35 ± 5%) will cause a delayed proteolysis of the voltage gated sodium channel, as measured by immunoblotting.[62] For this injury level, we observe a consistent and immediate decrease in spontaneous activity, consistent with a recent report that excitatory transmission is altered following mechanical injury in cultured neurons[21] (Figs. 5a, 5b). Our detailed analysis of calcium transients on an individual neuron basis revealed a significant decrease in network synchronization (Fig. 5c). These changes in spontaneous activity and synchronization persisted for 6 h. Functional connectivity was also reduced, and the network topology showed signs of damage or rewiring as the previously integrated network, consisting of a single interconnected module, broke off into multiple sub-modules suggesting a loss in long-range connectivity. Finally, excitatory tone was decreased relative to uninjured control cultures, consistent with a broad loss in activity and synchronization (Fig. 5c).

Broadly, these data show that mechanical injury to cortical neurons will incur immediate and broad disruptions in network behavior. However, finite element models suggest a wide range of *in vivo* brain deformations occur during concussion. As such, we also tested a less severe injury level (10 ± 4%). Distinct from studies at the moderate injury level, we observed no change in the network synchronization or excitatory tone (Figs. 5d–5f). Interestingly, the frequency of network-wide spontaneous oscillations significantly increased acutely after injury and returned to pre-stretch levels by 1 h.

Blocking Calpain Activation After Mechanical Injury to Cortical Neurons Restores Synchrony

Given the divergence in network activity changes that occur following mechanical injury *in vitro*, we focused our efforts on the mechanical injury level that produced a broader disruption in synchrony and functional connectivity. At this injury level, past studies show a calcium-activated neutral protease (calpain) is capable of cleaving the α-subunit of the voltage gated sodium channel.[52,62] Residing principally at the axon initial segment, cleavage of the α-subunit is capable of reducing the ability of the sodium channel to inactivate or, alternatively, increases the threshold for firing an action potential. Indeed, both the delayed inactivation and/or the increased firing threshold in the *in silico* model are capable of generating broad disruptions in network synchrony (Figs. 6a, 6b). Experimentally,

preventing the activation of calpain with MDL28170 significantly improved network synchrony ($p < 0.01$, Fig. 6c). Interestingly, blocking calcium influx with APV pre-treatment greatly attenuated the loss in synchronization, but it did not rescue it completely ($p = 0.0423$). This maybe due to the partial loss of NMDAR magnesium block and pathological activation of different NMDAR subtypes that then contribute to uncoordinated calcium transients.[54]

DISCUSSION

In this study, we assess fluorescence based imaging methods for mapping neural network properties, and use our analysis to design experiments for measuring changes in network behavior following mild mechanical injury to cortical neural networks *in vitro*. Unlike higher injury levels that will cause neuronal death within 24 h post-injury, we find that mild mechanical injury causes two different types of changes at the network level. At moderate *in vitro* injury levels (35% stretch), we find an acute loss in network synchrony, changes in the network topology, and reduction in the excitatory tone that is not recovered up to 6 h following injury. At mild levels of mechanical injury, we see a different response—the network shows an enhanced frequency in firing that returns to baseline within 1 h post-stretch and does not show any change in synchronization or excitatory tone. The more significant changes in network behavior at moderate stretch are influenced by NMDA receptor activation and subsequent proteolytic changes in the neuronal populations, as these changes would be attenuated significantly with NMDAR antagonists and, separately, a calpain inhibitor.

A number of recent efforts developed and characterized the ability of existing and new molecular probes to function as a surrogate indicator of single-cell electrical activity. These efforts are now positioned to probe network dynamics and complement traditional microelectrode array technologies. Our predictions of probe sensitivity, accuracy, and minimum detection thresholds for network topology are supported by measurements in parallel on dissociated cortical neuron networks. Similar to past work,[16,58] we find the relatively high speed imaging requirements restricts the use of probes to those with high efficiency and single emission capability—notably, Fluo-4 and some GCaMP variants. New contributions from our work include estimates for the number of neurons and the acquisition time period necessary to accurately capture descriptors of the network. These minimal imaging requirements will help set the framework for experiments where it may be useful to map the response of the network to any given stimulus. It is important to point out that our analysis assumed stability of the network topology during the imaging period. Certainly, any *in vitro* neural circuit exhibits the potential to change the strength, number, and degree of connections over time. The relatively short imaging periods needed to estimate network connectivity makes this approach ideal for studying changes in neural circuits that occur during development, in response to prolonged exposure to chemical treatment, or mechanical stimulus. Less ideal are conditions where the network changes in seconds; to our knowledge, there is no optical imaging technology available to perform such a rapid examination of the network and microelectrode arrays may be a more appropriate approach.

We used these optimized imaging algorithms to study changes in dissociated cortical neurons following mechanical injury. An emerging set of studies show immediate disruptions in the network activity following mechanical trauma. Cullen *et al.* show that a rapidly applied fluid shear stress was capable of disrupting spontaneous action potential firing within selected neurons,[27] and similar changes were observed when three-dimensional constructs were injured in pure shear.[12] Using organotypic hippocampal slice cultures, Morrison *et al.* demonstrate that sublethal biaxial stretch causes electrophysiological dysfunction in the CA1, CA3, and dentate gyrus and results in changes in short-term plasticity.[63] Similarly, a suppression in broad periodic calcium oscillations appeared following injury to dissociated cortical neurons, and this suppression in activity persisted 2 days following the initial injury and was accompanied with a change in the composition of synaptic glutamate receptors.[21] The recent results from Goforth *et al.* are most directly comparable to our tests using a moderate level of mechanical injury, where our results also show an immediate reduction in spontaneous activity. Moreover, we observed a similar reduction in the excitatory tone of the network post-injury, using a method distinct from the electrophysiological techniques employed by Goforth *et al.* By acquiring imaging information at higher imaging rates and performing individual cell-based analysis, our data also reveal new features of this response that included an emergence of numerous local modules within the network, reduction in the functional connectivity, and a broad loss in synchronization.

These new data suggest that mechanical trauma can immediately change the topology of a network. Less clear, though, is the origin or functional consequence of this change in network wiring. Individual neurons with numerous connections to neighboring neurons are often critical in setting the dynamics of the network, even though they may represent a small fraction of the network.[33] We do not know if mechanical injury selectively impairs these ‘driver nodes’ in the network, therefore dramatically reducing the network excitability or controllability, or if the mechanical injury affects individual neurons more uniformly. Answering this question may be a key next step, since approaches to restore network dynamics may differ if the focus is on a small subpopulation of neurons (i.e., the driver neurons) or the entire network. Similarly, the degradation of the network into smaller modules requires a closer examination because it may provide a mechanism for subpopulations to restore connections among its neighboring neurons before re-integrating into the larger network. Alternatively, the increased modularity may represent an adaptive response to facilitate rapid and robust response to different environmental cues,[2] a feature that may be useful to counter subsequent injuries or aid in the recovery process after injury.

Given past work showing that the NMDA receptor is a key glutamate mechanical sensor during injury, we were not surprised that blocking this mechanical sensor would help alleviate the effects of mechanical injury on the network. At this level of injury, we do not observe significant changes in the membrane permeability, often termed mechanoporation.[11,19,26] As such, the NMDAR emerges as the most likely contributor to neuronal dynamics following mechanical injury. Indeed, the nearly complete restoration of network synchrony with NMDAR inhibition suggests the NMDA receptor is a primary mechanistic pathway that can influence subsequent changes in the neural circuit behavior. The small reduction in synchrony, even with NMDAR blockade, may be due to calcium

activity from partial loss of magnesium block.[64] We also found that a downstream consequence of NMDAR activation—the activation of calpain—also appears critical in mediating the functional impairment observed in neural circuits after TBI. Past work shows that protease activation following mechanical injury is sufficient to cause breakdown of sodium channel sub-units in axons within minutes following mechanical injury,[22] and our data now suggest the effect of calpain can be even more rapid. The immediate influence of calpain activation suggests a critical role for this protease in the earliest phase after injury, where maintaining network synchrony may be important to promote or enhance pro-survival signaling through synaptic NMDARs. The impact of calpain disrupting the timing of neural circuitry may adversely affect any enhancement of prosurvival signaling through the NMDARs, as this signaling is strongly activated in highly synchronized networks.[29,47] This persisting loss in synchrony likely extends well beyond the initial phase of calcium influx and calpain activation, as turnover of sodium channels and insertion of new sodium channels is slow.[8] Therefore, defining the window of altered synchrony will be a key step in assessing recoverability of the network to mechanical injury. For example, persisting alterations in synchrony mediated by even transient calpain activation may also make it more difficult to establish network activity patterns that can lead to either synaptic strengthening or depotentiation, two key steps in cellular models of learning and memory. Alternatively, a loss in synchrony may limit the overexcitatory input that may appear in sustained, aberrant bursts of the network following trauma.

Taken together, these data point to new opportunities for merging information from different perspectives (*in silico* and *in vitro*) and length scales to study the dynamic state of neural circuits following traumatic mechanical injury. Although the emerging picture on mild mechanical injury to neural circuits remains to be fully developed, our studies suggest a broad continuum of responses in the network behavior. In addition, the ability to measure single neuronal properties from this network response will lead to a new understanding of the initiating injury mechanisms that influence the consequence of mechanical injury to *in vitro* networks, leading potentially to a better understanding of circuit dysfunction in mild traumatic brain injury.

Acknowledgments

We thank Dr. Pallab Singh (University of Pennsylvania) for providing NMDAR and AMPAR activation profiles and for helpful discussions that led to the development of our stochastic integrate-and-fire model. Funding for this work was provided from the National Institutes of Health and the Department of Defense (W911NF-10-1-0526).

References

1. Amit DJ, Brunel N. Model of global spontaneous activity and local structured activity during delay periods in the cerebral cortex. Cereb. Cortex. 1997; 7:237–252. [PubMed: 9143444]
2. Babu MM, Luscombe NM, Aravind L, Gerstein M, Teichmann SA. Structure and evolution of transcriptional regulatory networks. Curr. Opin. Struct. Biol. 2004; 14:283–291. [PubMed: 15193307]
3. Bialonski S, Lehnertz K. Identifying phase synchronization clusters in spatially extended dynamical systems. Phys. Rev. E Stat. Nonlin. Soft Matter Phys. 2006; 74:051909. [PubMed: 17279941]
4. Bottlang M, Sommers MB, Lusardi TA, Miesch JJ, Simon RP, Xiong ZG. Modeling neural injury in organotypic cultures by application of inertia-driven shear strain. J. Neurotrauma. 2007; 24:1068–1077. [PubMed: 17600521]

5. Breskin I, Soriano J, Moses E, Tlusty T. Percolation in living neural networks. Phys. Rev. Lett. 2006; 97(18):188102. [PubMed: 17155581]
6. Browne KD, Chen XH, Meaney D, Smith DH. Mild traumatic brain injury and diffuse axonal injury in swine. J. Neurotrauma. 2011; doi: 10.1089/neu.2011.1913
7. Bullmore E, Sporns O. Complex brain networks: graph theoretical analysis of structural and functional systems. Nat. Rev. Neurosci. 2009; 10:186–198. [PubMed: 19190637]
8. Cantrell AR, Catterall WA. Neuromodulation of Na+ channels: an unexpected form of cellular plasticity. Nat. Rev. Neurosci. 2001; 2:397–407. [PubMed: 11389473]
9. Cao C, Slobounov S. Alteration of cortical functional connectivity as a result of traumatic brain injury revealed by graph theory, ICA, and sLORETA analyses of EEG signals. IEEE Trans. Neural Syst. Rehabil. Eng. 2010; 18:11–19. [PubMed: 20064767]
10. Church AJ, Andrew RD. Spreading depression expands traumatic injury in neocortical brain slices. J. Neurotrauma. 2005; 22:277–290. [PubMed: 15716633]
11. Cullen DK, LaPlaca MC. Neuronal response to high rate shear deformation depends on heterogeneity of the local strain field. J. Neurotrauma. 2006; 23:1304–1319. [PubMed: 16958583]
12. Cullen DK, Lessing MC, LaPlaca MC. Collagen-dependent neurite outgrowth and response to dynamic deformation in three-dimensional neuronal cultures. Ann. Biomed. Eng. 2007; 35:835–846. [PubMed: 17385044]
13. Dev KK, Petersen V, Honore T, Henley JM. Pharmacology and regional distribution of the binding of 6-[3H]nitro-7-sulphamoylbenzo[f]-quinoxaline-2,3-dione to rat brain. J. Neurochem. 1996; 67:2609–2612. [PubMed: 8931496]
14. Difiori JP, Giza CC. New techniques in concussion imaging. Curr. Sports Med. Rep. 2010; 9:35–39. [PubMed: 20071919]
15. Dombeck DA, Harvey CD, Tian L, Looger LL, Tank DW. Functional imaging of hippocampal place cells at cellular resolution during virtual navigation. Nat. Neurosci. 2010; 13:1433–1440. [PubMed: 20890294]
16. Fetcho JR, Cox KJ, O'Malley DM. Monitoring activity in neuronal populations with single-cell resolution in a behaving vertebrate. Histochem. J. 1998; 30:153–167. [PubMed: 10188924]
17. French DA, Gruenstein EI. An integrate-and-fire model for synchronized bursting in a network of cultured cortical neurons. J. Comput. Neurosci. 2006; 21:227–241. [PubMed: 16951925]
18. Garofalo M, Nieus T, Massobrio P, Martinoia S. Evaluation of the performance of information theory-based methods and cross-correlation to estimate the functional connectivity in cortical networks. PLoS ONE. 2009; 4(8):e6482. [PubMed: 19652720]
19. Geddes-Klein DM, Schiffman KB, Meaney DF. Mechanisms and consequences of neuronal stretch injury in vitro differ with the model of trauma. J. Neurotrauma. 2006; 23:193–204. [PubMed: 16503803]
20. Geddes-Klein DM, Serbest G, Mesfin MN, Cohen AS, Meaney DF. Pharmacologically induced calcium oscillations protect neurons from increases in cytosolic calcium after trauma. J. Neurochem. 2006; 97:462–474. [PubMed: 16539664]
21. Goforth PB, Ren J, Schwartz BS, Satin LS. Excitatory synaptic transmission and network activity are depressed following mechanical injury in cortical neurons. J. Neurophysiol. 2011; 105:2350–2363. [PubMed: 21346214]
22. Iwata A, Stys PK, Wolf JA, Chen XH, Taylor AG, Meaney DF, Smith DH. Traumatic axonal injury induces proteolytic cleavage of the voltage-gated sodium channels modulated by tetrodotoxin and protease inhibitors. J. Neurosci. 2004; 24:4605–4613. [PubMed: 15140932]
23. Kamioka H, Maeda E, Jimbo Y, Robinson HP, Kawana A. Spontaneous periodic synchronized bursting during formation of mature patterns of connections in cortical cultures. Neurosci. Lett. 1996; 206:109–112. [PubMed: 8710163]
24. Kraus JF, Nourjah P. The epidemiology of mild, uncomplicated brain injury. J. Trauma. 1988; 28:1637–1643. [PubMed: 3199464]
25. LaPlaca MC, Cullen DK, McLoughlin JJ, Cargill RS. High rate shear strain of three-dimensional neural cell cultures: a new in vitro traumatic brain injury model. J. Biomech. 2005; 38:1093–1105. [PubMed: 15797591]

26. Laplaca MC, Prado GR. Neural mechanobiology and neuronal vulnerability to traumatic loading. J. Biomech. 2010; 43:71–78. [PubMed: 19811784]
27. LaPlaca MC, Prado GR, Cullen DK, Irons HR. High rate shear insult delivered to cortical neurons produces heterogeneous membrane permeability alterations. Conf. Proc. IEEE Eng. Med. Biol. Soc. 2006; 1:2384–2387. [PubMed: 17946956]
28. LaPlaca MC, Thibault LE. An in vitro traumatic injury model to examine the response of neurons to a hydrodynamically-induced deformation. Ann. Biomed. Eng. 1997; 25:665–677. [PubMed: 9236979]
29. Leveille F, Papadia S, Fricker M, Bell KFS, Soriano FX, Martel MA, Puddifoot C, Habel M, Wyllie DJ, Ikonomidou C, Tolkovsky AM, Hardingham GE. Suppression of the intrinsic apoptosis pathway by synaptic activity. J. Neurosci. 2010; 30:2623–2635. [PubMed: 20164347]
30. Li XL, Cui D, Jiruska P, Fox JE, Yao X, Jefferys JGR. Synchronization measurement of multiple neuronal populations. J. Neurophysiol. 2007; 98:3341–3348. [PubMed: 17913983]
31. Li X, Ouyang G, Usami A, Ikegaya Y, Sik A. Scale-free topology of the CA3 hippocampal network: a novel method to analyze functional neuronal assemblies. Biophys. J. 2010; 98:1733–1741. [PubMed: 20441736]
32. Lin YC, Huang ZH, Jan IS, Yeh CC, Wu HJ, Chou YC, Chang YC. Development of excitatory synapses in cultured neurons dissociated from the cortices of rat embryos and rat pups at birth. J. Neurosci. Res. 2002; 67:484–493. [PubMed: 11835315]
33. Liu YY, Slotine JJ, Barabasi AL. Controllability of complex networks. Nature. 2011; 473:167–173. [PubMed: 21562557]
34. Lusardi TA, Rangan J, Sun D, Smith DH, Meaney DF. A device to study the initiation and propagation of calcium transients in cultured neurons after mechanical stretch. Ann. Biomed. Eng. 2004; 32:1546–1558. [PubMed: 15636114]
35. Lusardi TA, Wolf JA, Putt ME, Smith DH, Meaney DF. Effect of acute calcium influx after mechanical stretch injury in vitro on the viability of hippocampal neurons. J. Neurotrauma. 2004; 21:61–72. [PubMed: 14987466]
36. Meaney DF, Smith DH. Biomechanics of concussion. Clin. Sports Med. 2011; 30:19–31. vii. [PubMed: 21074079]
37. Mittmann W, Wallace DJ, Czubayko U, Herb JT, Schaefer AT, Looger LL, Denk W, Kerr JN. Two-photon calcium imaging of evoked activity from L5 somatosensory neurons in vivo. Nat. Neurosci. 2011; 14(8):1089–1093. [PubMed: 21743473]
38. Morrison B, Elkin BS, Dolle JP, Yarmush ML. In vitro models of traumatic brain injury. Annu. Rev. Biomed. Eng. 2011; 13:91–126. [PubMed: 21529164]
39. Morrison B 3rd, Meaney DF, McIntosh TK. Mechanical characterization of an in vitro device designed to quantitatively injure living brain tissue. Ann. Biomed. Eng. 1998; 26:381–390. [PubMed: 9570221]
40. Morrison B 3rd, Saatman KE, Meaney DF, McIntosh TK. In vitro central nervous system models of mechanically induced trauma: a review. J. Neurotrauma. 1998; 15:911–928. [PubMed: 9840765]
41. Mukhin AG, Ivanova SA, Allen JW, Faden AI. Mechanical injury to neuronal/glial cultures in microplates: role of NMDA receptors and pH in secondary neuronal cell death. J. Neurosci. Res. 1998; 51:748–758. [PubMed: 9545088]
42. Mukhin AG, Ivanova SA, Knoblach SM, Faden AI. New in vitro model of traumatic neuronal injury: evaluation of secondary injury and glutamate receptor-mediated neurotoxicity. J. Neurotrauma. 1997; 14:651–663. [PubMed: 9337127]
43. Murphy EJ, Horrocks LA. A model for compression trauma: pressure-induced injury in cell cultures. J. Neurotrauma. 1993; 10:431–444. [PubMed: 8145266]
44. Nenadic Z, Burdick JW. Spike detection using the continuous wavelet transform. IEEE Trans. Biomed. Eng. 2005; 52:74–87. [PubMed: 15651566]
45. Newman ME. Modularity and community structure in networks. Proc. Natl Acad. Sci. USA. 2006; 103:8577–8582. [PubMed: 16723398]

46. Ommaya AK, Gennarelli TA. Cerebral concussion and traumatic unconsciousness. Correlation of experimental and clinical observations of blunt head injuries. Brain. 1974; 97:633–654. [PubMed: 4215541]
47. Papadia S, Soriano FX, Léveillé F, Martel M-A, Dakin KA, Hansen HH, Kaindl A, Sifringer M, Fowler J, Stefovska V, McKenzie G, Craigon M, Corriveau R, Ghazal P, Horsburgh K, Yankner BA, Wyllie DJA, Ikonomidou C, Hardingham GE. Synaptic NMDA receptor activity boosts intrinsic antioxidant defenses. Nat. Neurosci. 2008; 11:476–487. [PubMed: 18344994]
48. Pardo E, San Emeterio JL, Rodriguez MA, Ramos A. Noise reduction in ultrasonic NDT using undecimated wavelet transforms. Ultrasonics. 2006; 44(Suppl 1):e1063–e1067. [PubMed: 16797651]
49. Pfister BJ, Weihs TP, Betenbaugh M, Bao G. An in vitro uniaxial stretch model for axonal injury. Ann. Biomed. Eng. 2003; 31:589–598. [PubMed: 12757202]
50. Rubinov M, Sporns O. Complex network measures of brain connectivity: uses and interpretations. NeuroImage. 2010; 52:1059–1069. [PubMed: 19819337]
51. Rummel C, Muller M, Schindler K. Data-driven estimates of the number of clusters in multivariate time series. Phys. Rev. E Stat. Nonlin. Soft Matter Phys. 2008; 78:066703. [PubMed: 19256977]
52. Saatman KE, Abai B, Grosvenor A, Vorwerk CK, Smith DH, Meaney DF. Traumatic axonal injury results in biphasic calpain activation and retrograde transport impairment in mice. J. Cereb. Blood Flow Metab. 2003; 23:34–42. [PubMed: 12500089]
53. Sieg F, Wahle P, Pape HC. Cellular reactivity to mechanical axonal injury in an organotypic in vitro model of neurotrauma. J. Neurotrauma. 1999; 16:1197–1213. [PubMed: 10619198]
54. Singh P, Hockenberry AJ, Tiruvadi VR, Meaney DF. Computational investigation of the changing patterns of subtype specific NMDA receptor activation during physiological glutamatergic neurotransmission. PLoS Comput. Biol. 2011; 7:e1002106. [PubMed: 21738464]
55. Smith DH, Nonaka M, Miller R, Leoni M, Chen XH, Alsop D, Meaney DF. Immediate coma following inertial brain injury dependent on axonal damage in the brainstem. J. Neurosurg. 2000; 93:315–322. [PubMed: 10930019]
56. Spaethling JM, Klein DM, Singh P, Meaney DF. Calcium-permeable AMPA receptors appear in cortical neurons after traumatic mechanical injury and contribute to neuronal fate. J. Neurotrauma. 2008; 25:1207–1216. [PubMed: 18986222]
57. Stam CJ, Reijneveld JC. Graph theoretical analysis of complex networks in the brain. Nonlinear Biomed. Phys. 2007; 1:3. [PubMed: 17908336]
58. Stosiek C, Garaschuk O, Holthoff K, Konnerth A. In vivo two-photon calcium imaging of neuronal networks. Proc. Natl Acad. Sci. USA. 2003; 100:7319–7324. [PubMed: 12777621]
59. Takahashi N, Sasaki T, Usami A, Matsuki N, Ikegaya Y. Watching neuronal circuit dynamics through functional multineuron calcium imaging (fMCI). Neurosci. Res. 2007; 58:219–225. [PubMed: 17418439]
60. Tian L, Hires SA, Mao T, Huber D, Chiappe ME, Chalasani SH, Petreanu L, Akerboom J, McKinney SA, Schreiter ER, Bargmann CI, Jayaraman V, Svoboda K, Looger LL. Imaging neural activity in worms, flies and mice with improved GCaMP calcium indicators. Nat. Methods. 2009; 6:875–881. [PubMed: 19898485]
61. van Vreeswijk C, Sompolinsky H. Chaos in neuronal networks with balanced excitatory and inhibitory activity. Science. 1996; 274:1724–1726. [PubMed: 8939866]
62. von Reyn CR, Spaethling JM, Mesfin MN, Ma M, Neumar RW, Smith DH, Siman R, Meaney DF. Calpain mediates proteolysis of the voltage-gated sodium channel alpha-subunit. J. Neurosci. 2009; 29:10350–10356. [PubMed: 19692609]
63. Yu Z, Morrison B 3rd. Experimental mild traumatic brain injury induces functional alteration of the developing hippocampus. J. Neurophysiol. 2010; 103:499–510. [PubMed: 19923245]
64. Zhang L, Rzigalinski BA, Ellis EF, Satin LS. Reduction of voltage-dependent Mg2+ blockade of NMDA current in mechanically injured neurons. Science. 1996; 274:1921–1923. [PubMed: 8943207]

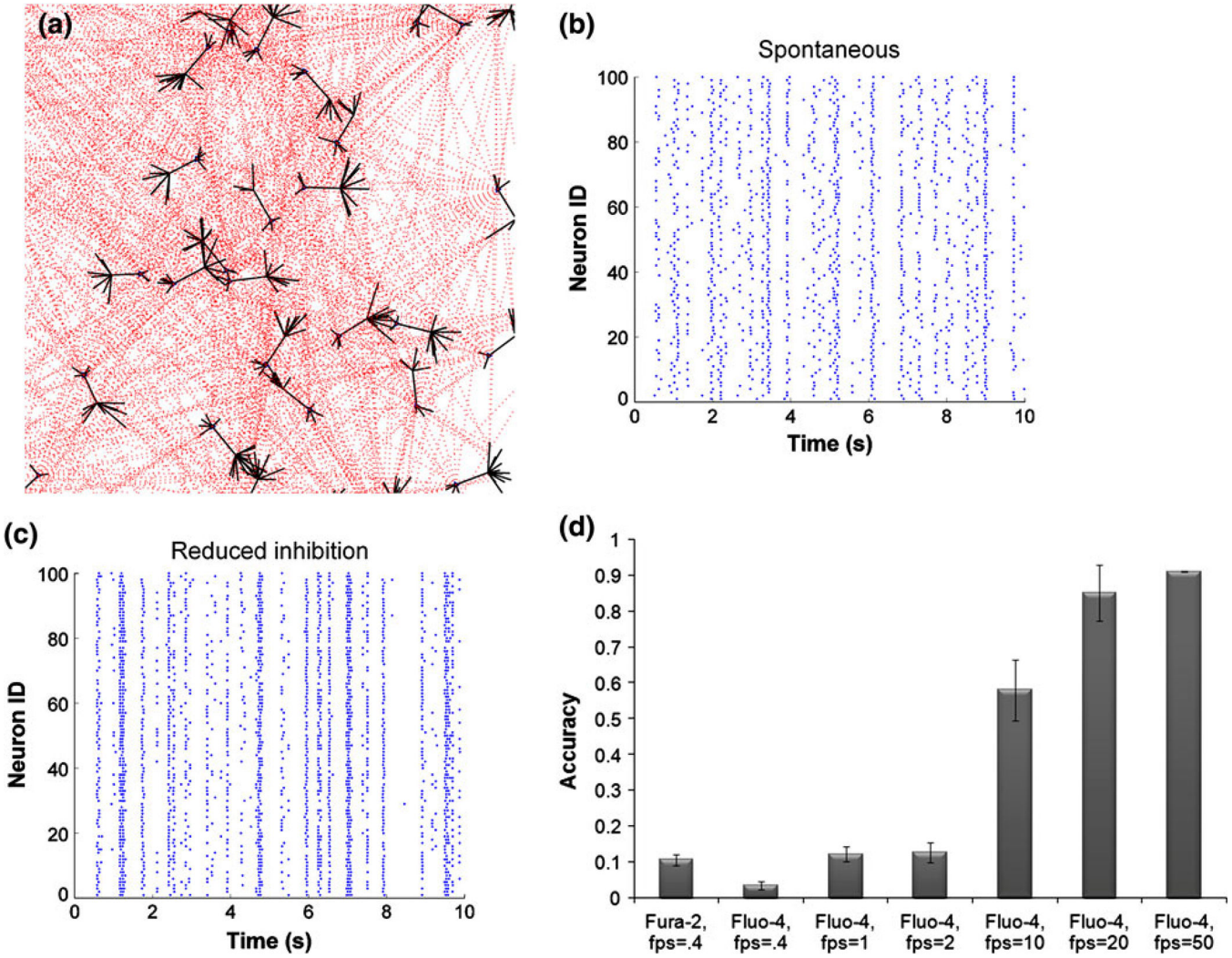

Figure 1. ***In silico*** **model of neural network activity**

(a) Pyramidal excitatory neuronal network was constructed, where each neuron connected to 20 other neurons on average, chosen from a Poisson distribution. Synaptic connections occurred on dendritic spines, populated with AMPA and NMDA receptors. (b, c) Stochastic integrate-and-fire model reproduced spontaneous activity patterns, composed of flickering events, intermixed with network-wide bursts. Reducing the strength of the inhibitory network increased synchronous oscillations. (d) Calcium transients predicted from underlying action potentials were converted to fluorescence traces for fura-2 and fluo-4, taking into account their unique buffering properties. The accuracy of resolving action potentials using fluorescent dye is greater for fluo-4 and increases with imaging acquisition speed.

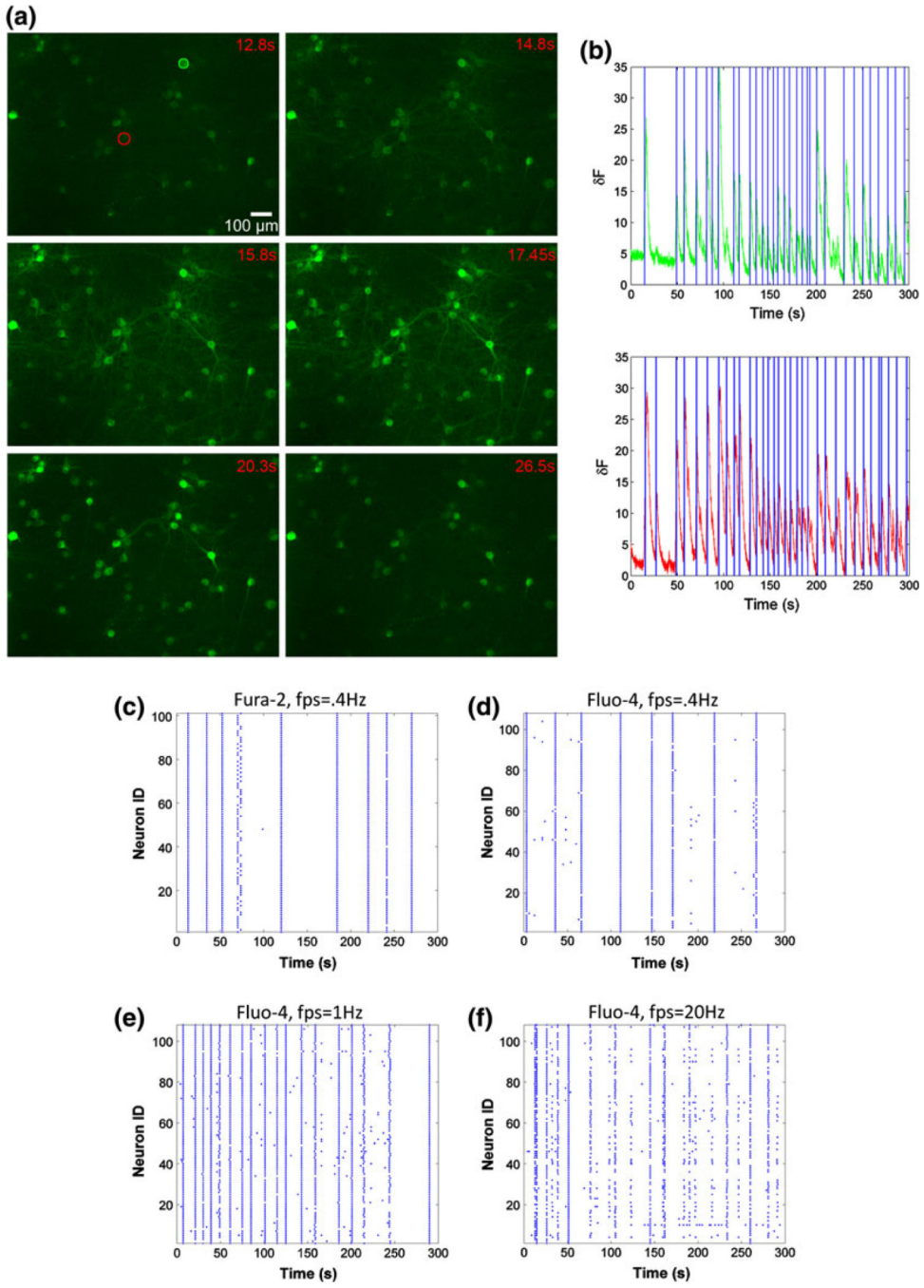

Figure 2. Comparison of *in vitro* calcium imaging with fura-2, fluo-4 and GCaMP3 at varying frame rates

(a) Time-lapse image of GCaMP-3 transduced cortical neurons captured during a network-wide burst event (20 frames per second acquisition speed). (b) Fluorescence trace of two ROIs across 5 min acquisition. Onsets of calcium transients were automatically detected using a continuous-wavelet transform with >98% accuracy compared to manual detection. (c, d) Representative examples of spontaneous activity of a mature culture (DIV 18), captured with fura-2 and fluo-4 at the same acquisition speed. The same fluo-4 loaded

culture was imaged at higher speeds (e, 1 Hz) and (f, 20 Hz), revealing richer network activity patterns.

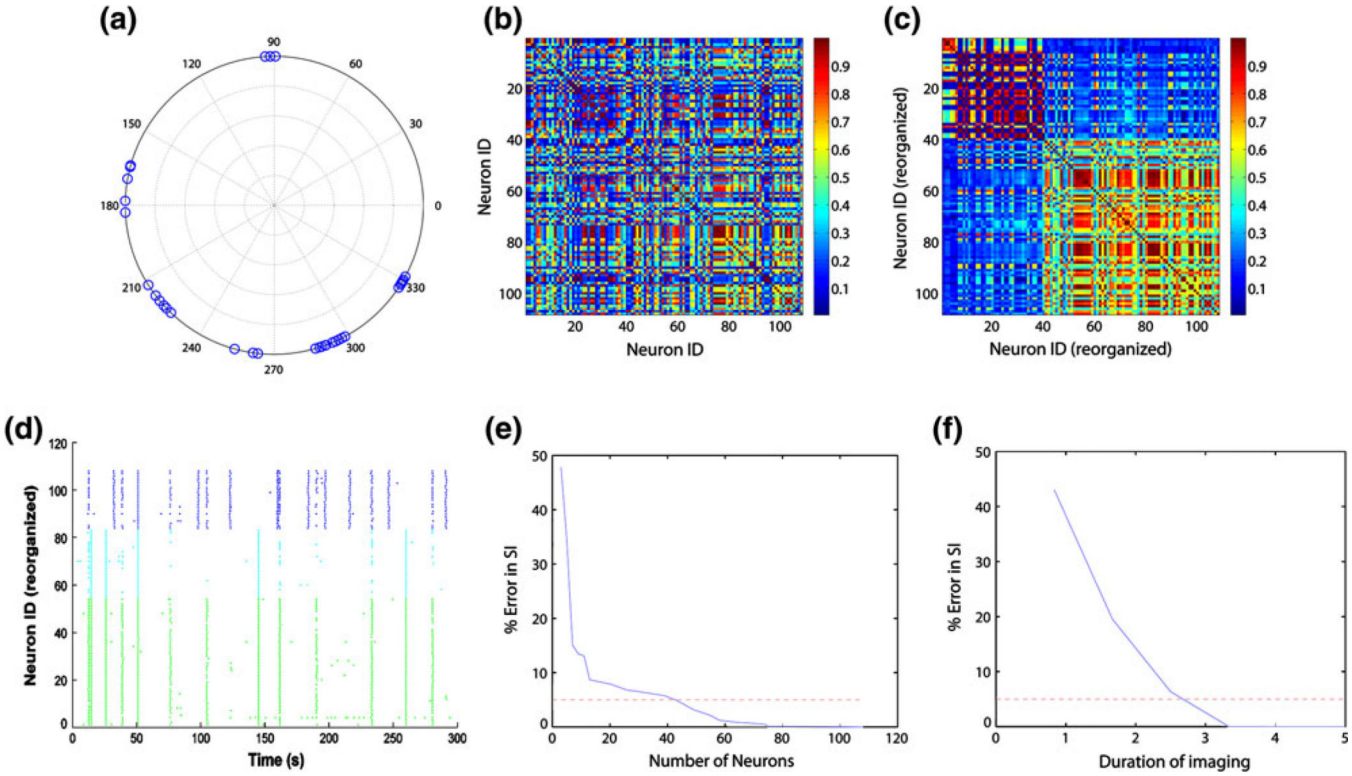

Figure 3. Synchronization analysis for the calcium activity in Fig 2f

The instantaneous phase for each neuron's calcium activity (a) was used to compute pair-wise phase synchronization index (b). An eigen-vector based algorithm identified 3 clusters of synchronously oscillating neurons (c, neuron IDs rearranged by cluster assignment, global synchronization index: 0.4304). (d) The raster plot of activity from Fig. 2f is rearranged and color-coded by the 3 identified clusters. e Repeated sampling of fraction of neurons in the field of view show that at least 40 neurons need to be imaged to achieve <5% error in synchronization measurement. (f) Similarly, at least 2.5 min imaging duration yields <5% error.

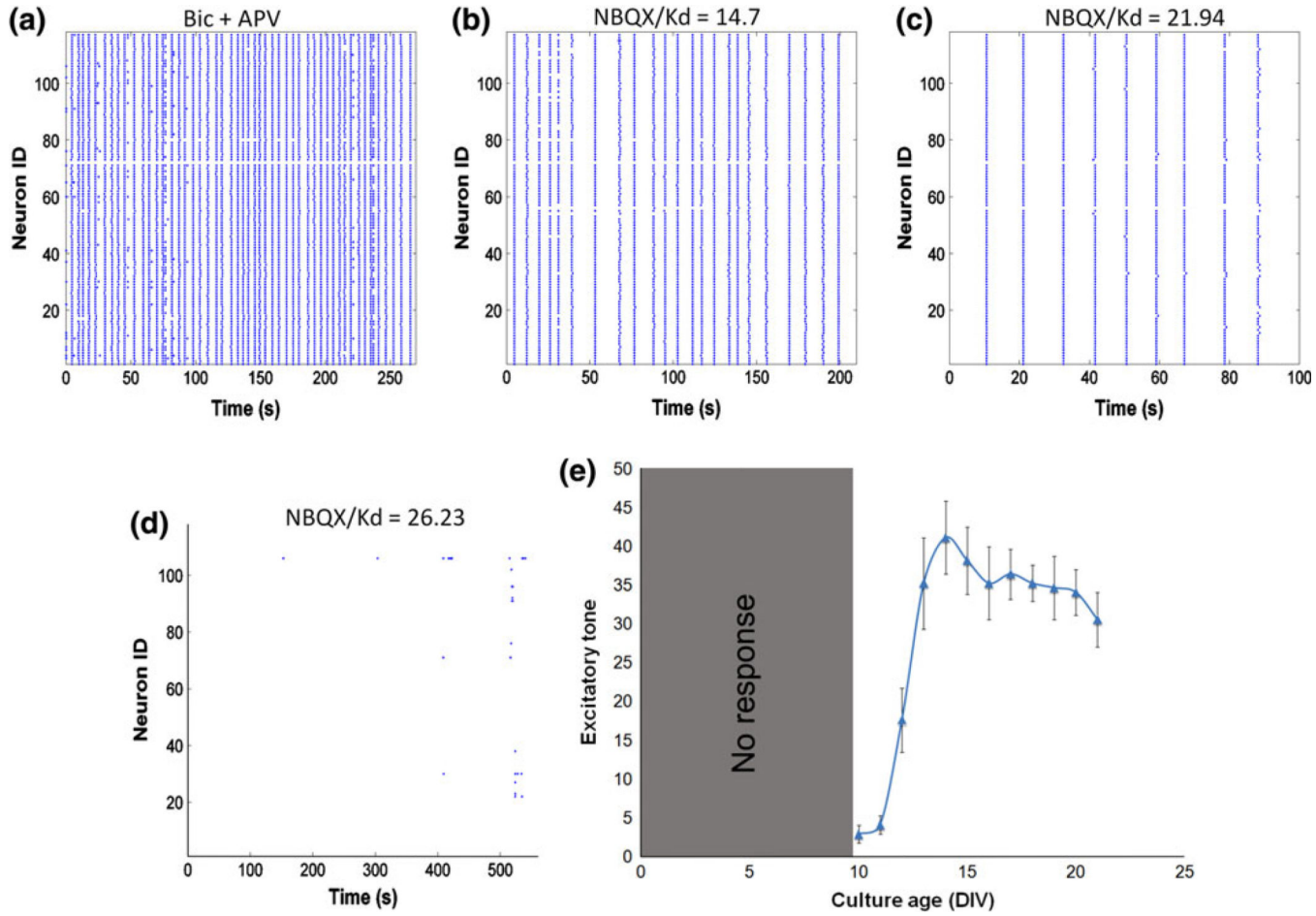

Figure 4. Excitatory tone measurement

Forced oscillations were induced by network disinhibition with bicuculline (a). Progressive application of increasing [NBQX] decreased the frequency of oscillations until a critical threshold was reached when synchronous activity abruptly stopped (b–d). The excitatory tone increases as neurons mature in culture (e).

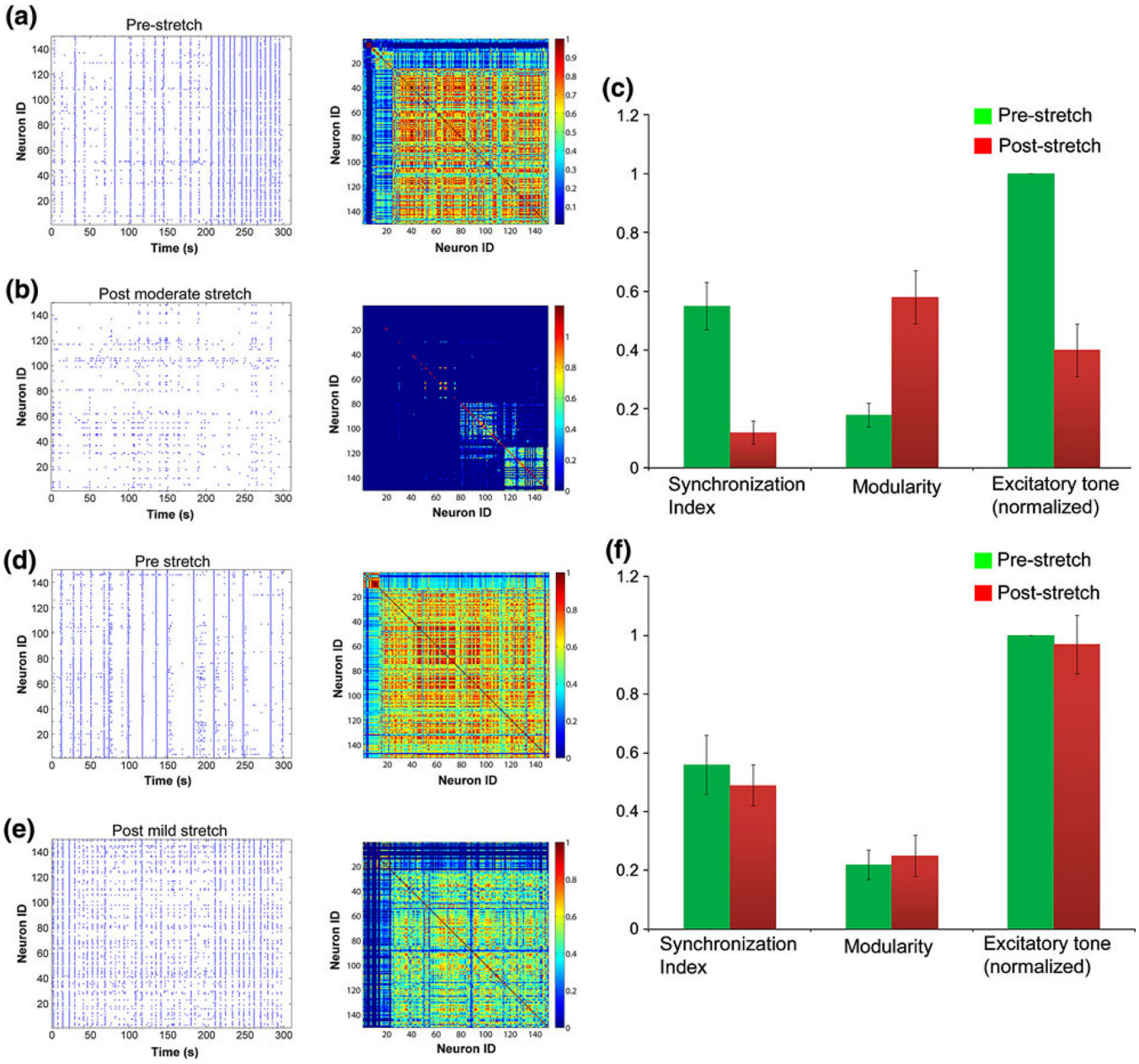

Figure 5. Changes in network activity following 35 and 10% mechanical stretch

The spontaneous activity of a mature culture is greatly reduced and de-synchronized 1 h after 35% stretch (a, b). There is a significant drop in global synchronization and excitatory tone ($p < 0.01$) and an increase in modularity of the network (c). Alternatively, network activity is unaltered after 10% stretch and shows a transient period of heightened activity (d, e). Synchronization, modularity and excitatory tone remain unchanged after 10% stretch (f).

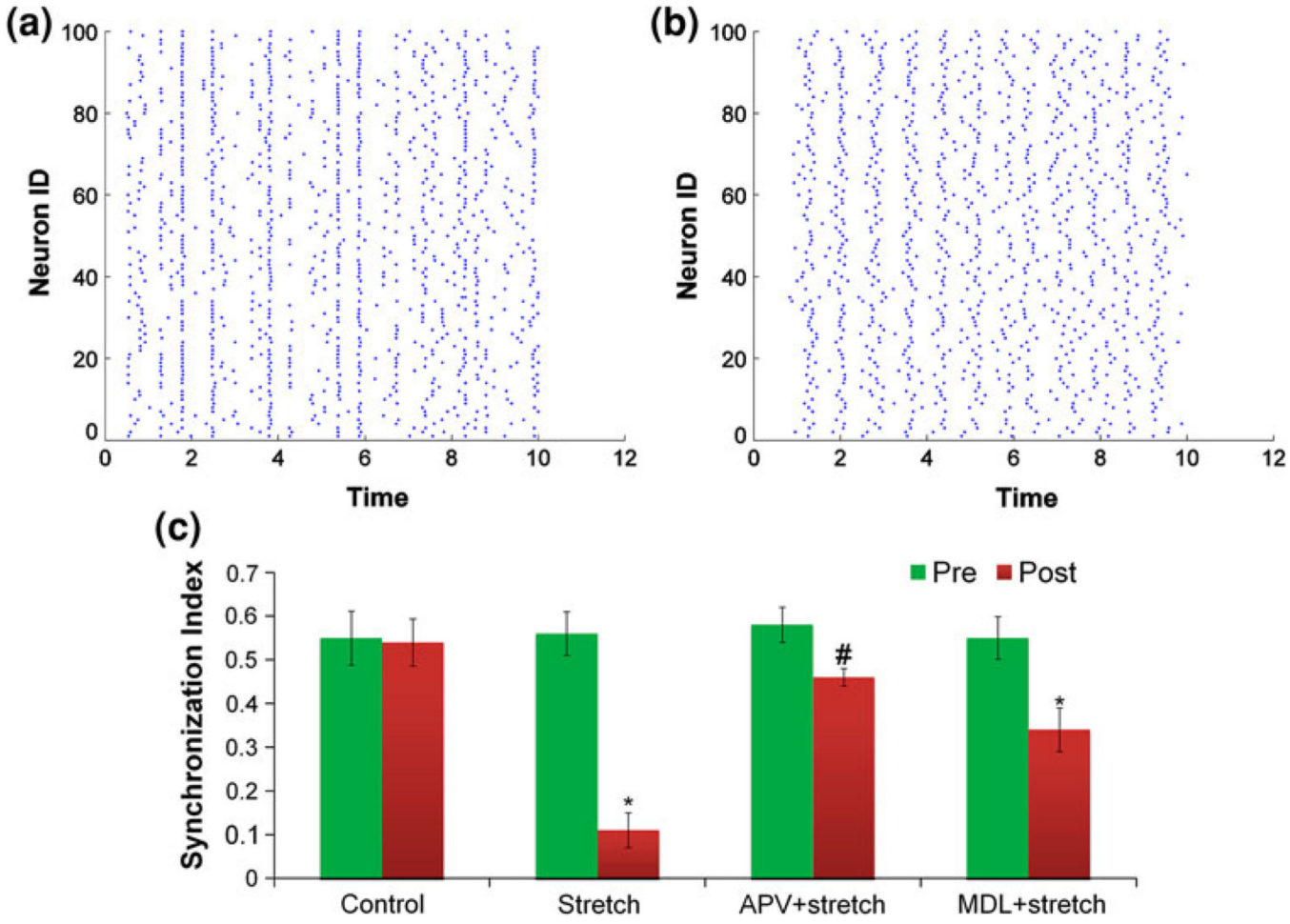

Figure 6. Rescuing synchronization

Using our *in silico* model, we show that axonal pathology can significantly reduce synchronization ((a) pre-simulated pathology, (b) post-simulated pathology). Blocking calcium entry with APV or calpain activation with MDL28170 significantly attenuate the loss in synchronization, following 35% stretch (*p<0.01, #p<0.05) (c).

Table 1

Properties of two commonly used calcium indicator dyes.

	Fura-2	**Fluo-4**
K_d	145 nM	345 nM
R_{min}	0.3982	121
R_{max}	2.7021	549
Frame rate	0.4 Hz	0.4–20 Hz